OPEN ACCESS
Freely Available Online

JOURNAL OF ADVANCES IN NANOTECHNOLOGY
ISSN NO: 2689-2855

Research

DOI: 10.14302/issn.2689-2855.jan-19-2744

Investigation of Edge-Selectively Nitrogen-Doped Metal Free Graphene for Oxygen Reduction Reaction

Huan He[1], Qingwei Yang[1], Shaohua Xiao[1], Xiaoyan Han[1], Qin Li[1], Kangle Lv[1], Jingping Hong[1], Dingguo Tang[1], Deng Kejian[1,*]

[1]Key Laboratory of Catalysis and Materials Sciences of the State Ethnic Affairs Commission & Ministry of Education, South-Central University for Nationalities, Wuhan, 430074, Hubei, China

Abstract

In order to distinguish the roles of four types of nitrogen species in oxygen reduction reaction, the ketoamine condensation reactions between the ketone group of graphene oxide and amidogen of aniline and o-phenylenediamine were employed to generate –C=N- bond at the edge of graphene nanoplatelets, and then nitrogen-doped graphene nanoplatelets with pyrrolic N, pyridinic N and pyridinic N+-O- rather than graphitic nitrogen were obtained by post thermal treatments. The resulting catalysts were characterized by X-ray diffraction analysis, X-ray photoelectron spectroscopy and electrochemical measurements. It is found that edge-selectively nitrogen-doped graphene nanopaltelets with nitrogen content of up to 4.28 atom% have been prepared. Nitrogen doping helps to improve activity of oxygen reduction reaction slightly, suggesting nitrogen doping at the edge of graphene does not contribute a lot to the enhancement of activity.

Corresponding author: Deng Kejian, Key Laboratory of Catalysis and Materials Sciences of the State Ethnic Affairs Commission & Ministry of Education, South-Central University for Nationalities, Wuhan, 430074, Hubei, China. Email: dengkj@scuec.edu.cn

Keywords: Edge selectivity, Nitrogen doping, Graphene, Oxygen reduction reaction, Ketoamine condensation reaction

Received: Mar 28, 2019 **Accepted:** Jan 04, 2020 **Published:** Jan 09, 2020

Editor: Huang Haitao, Applied Physics Department, Hong Kong Poly, Hong Kong.

Introduction

Fuel cells are electrochemical energy device which converts chemical energy into electricity directly. Due to their distinguished features, such as high energy efficiency, zero-pollution, and silence, fuel cells are expected to be alternative solutions for the power supply for mobile applications or the combination of heat and power sources for stationary devices [1]. However, the sluggish kinetics of electrochemical processes like oxygen reduction reaction (ORR) is recognized as one of the challenges which hinder the developments of fuel cells. Noble metal catalysts contribute to boosting the reaction kinetics but inhibit their extensive commercial use due to their scarcity and high price.

Accordingly, metal-free carbon-based catalysts for ORR have attracted much attention as a promising non-precious-metal alternative to the conventional Pt-based catalysts [2,3]. Carbon materials doping with Nitrogen were found to show superior activity and stability for ORR. The net positive charge resulting from the heteroatom doping may effectively cause active sites to reduce the chemisorption's over potential of oxygen, enhancing the ORR activity of carbon materials [4]. N-doped carbon nanomaterials have been explored to be effective electro-catalysts for ORR. The N-doped carbon nanomaterials were usually synthesized in the presence of ammonia or precursor containing nitrogen [5]. Uncontrollable carbonization and doping always happen at the same time. The exact catalytic role for each of the nitrogen forms in carbon based ORR catalysts is still a matter of controversy [6]. Several researchers reported that the pyridinic N can enhance ORR activity of the N-doped carbon materials [7], while some others suggested that graphitic nitrogen atoms rather than the pyridinic ones are more important for ORR [8,9]. If graphene oxide (GO) with –C=N- bond is employed to generate N-doped graphene, the behavior of doping may be controllable, because the structure of graphene and –C=N- bond are stable during the carbonization. Controllable doping process would be very important to the investigation of ORR activity of N-doping graphene nanoplatelets [10,11].

In this work, the ketoamine condensation reaction was employed to generate –C=N- bond selectively at the edge of GO between the ketone group of GO and amidogen [12]. The precise control of N-doping and the precise synthesis of N-doped graphene nanoplatelets with specific chemical state of nitrogen atoms are available, and the further investigation of the ORR activity of N-doped graphene has been discussed below in detail [13].

Experimental

Synthesis of Catalyst

The N-doped graphene catalysts were prepared as follows [12]: GO was prepared by the modified Hummers' method using graphite nanopowders (AR, Sinopharm Chemical Reagent Co., Ltd). As shown in Scheme 1, for the preparation of iGO, GO (1 g) was dispersed in an acetic acid (140 mL)/toluene (30 mL) mixture via sonication for 1 h. Then, aniline (1 g, AR, Sinopharm Chemical Reagent Co., Ltd) was added into the mixture and heated under reflux with stirring overnight. Water formed during the dehydration reaction was completely removed automatically by using Dean–Stark trap. After cooling down to room temperature, the mixture was filtered by a PVDF (Polyvinylidene Fluoride) membrane (0.2 μm) and washed with plenty of methanol. The product was further purified by Soxhlet extraction with methanol and THF. iGO was obtained as a black powder after drying under reduced pressure at 60 °C overnight. Similarly, pGO was prepared via the same procedures using o-phenylenediamine (1 g, AR, Sinopharm Chemical Reagent Co., Ltd) instead of aniline. hiGO and hpGO were obtained by heat treatment of iGO and pGO at 900 °C under nitrogen atmosphere for 2 h.

Characterization of Catalyst

X-ray diffraction (XRD) patterns were recorded using a Bruker Advanced D8 diffraction instrument with monochromatized Cu K_α radiation (λ = 0.154056 nm) equipped with a VANTEC-1 detector in the 2θ range from 5° to 80° at scan rate of 10° min−1. X-ray photoelectron spectra (XPS) were performed on Multilab 2000 XPS system with a dual anode Al K_α source. Spectra were calibrated according to the C1s (284.6 eV) peak.

Electrochemical measurements were performed on a CHI (760E) electrochemical station equipped with a rotating disk electrode (RDE) system (MSR) in a conventional three-electrode cell at room

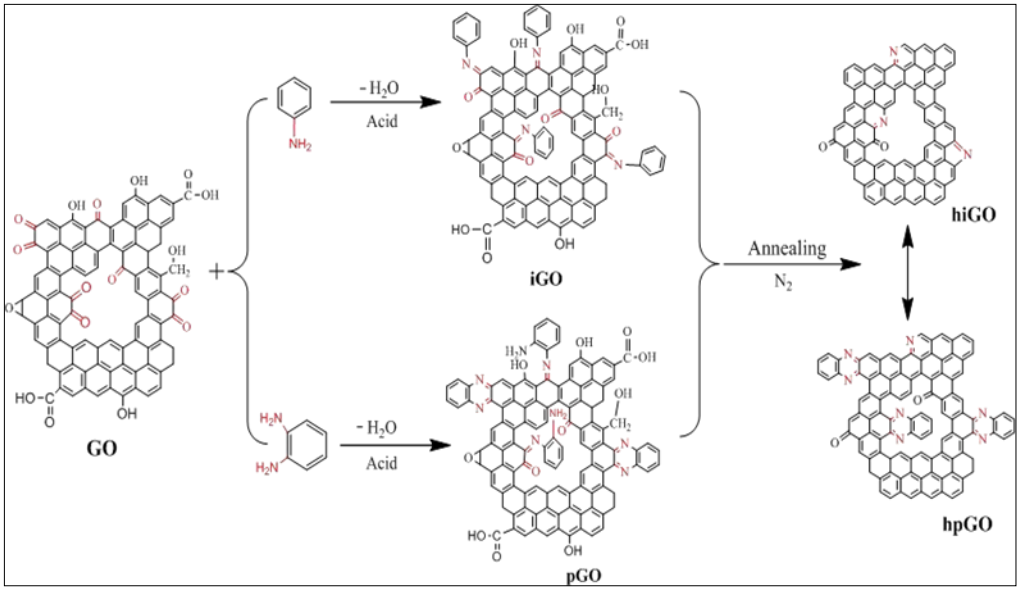

Scheme 1. Schematic representations of N-doping processes of N-doped graphene preparation via the condensation reaction between monoketone of graphene oxide and amidogen of aniline or o-phenylenediamine.

temperature. Glassy carbon electrode (0.19625 cm^2) coated with catalysts, Pt foil and Hg/HgO electrode (1 mol/L KOH) were used as the working electrode, counter electrode, and reference electrode, respectively. 5 mg of N-doped graphene catalyst and 50 µL of 5 wt% Nafion® solution were dispersed ultrasonically in 1 mL isopropanol for 30 minutes to form homogeneous slurry. Then, 20 µL of the slurry was transferred onto the glassy carbon electrode with a catalyst loading of 0.51 mg/cm^2 [14].

All electrochemical measurements were carried out in 0.1 M KOH and nitrogen or oxygen was used to purge the electrolyte to achieve oxygen-free or oxygen-saturated electrolyte solution. Linear sweep voltammogram (LSV) was conducted from 0.1 V to – 0.6 V at scan rate of 5 mV/s, and the rotating speed was 1600 rpm. All potentials were expressed towards Hg/HgO electrode (1 mol/L KOH) [12].

Results and Discussion

Physicalchemical Characterizations of N-Doped Graphene Catalysts

The powder X-ray diffraction (XRD) patterns of all samples are shown in Figure 1. The pristine graphite shows a sharp strong peak at ca. 26.4 ° and 42.5 °, which are attributed to (002) basal plane diffraction along the graphitic structure and (101) planes of graphitic C (Figure 1 (a)) [15]. By contrast, GO displays a weak and sharp peak at 2θ = 11.7 °, corresponding to an interlayer distance of 0.812 nm [12]. The increase in d-spacing of GO is ascribed to lattice expansion by oxygenated functional groups and bound small molecules between layers. Regardless of the way of Nitrogen doping, all the N-doped graphene catalysts show two peaks centered at ca. 26.4 ° and 42.5 ° (Figure 1 (b)). Moreover, the broad peak for iGO is significantly shifted to 24.1 ° (d-spacing ~ 0.369 nm), and the sharper and narrower peak for pGO is slightly shifted to 25.9 ° (d-spacing ~ 0.344 nm), which are consistent with small peak at ca. 9.5 ° for iGO and ca. 11.7 ° for pGO. Compared with d-spacing of pristine graphite (d-spacing ~ 0.337 nm), 0.344 nm for pGO is very close, indicating that spontaneous reduction and the formation of aromatic pyrazine rings have occurred [12]. After thermal treatments, the peak of hiGO or hpGO was shifted back to 26.4 ° (d-spacing ~ 0.337 nm), indicating that ketoamine condensation reactions and post-heat treatments are effective methods for the preparation of well-ordered N-doped graphene nanoplatelets [12, 16].

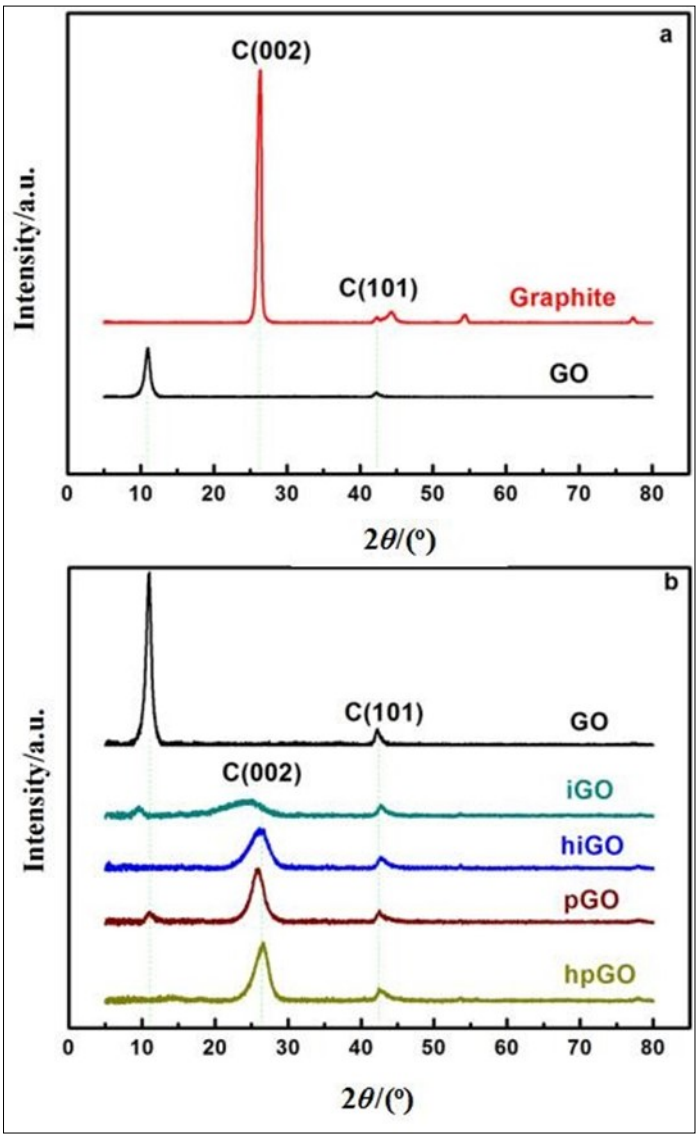

Figure 1. (a) XRD patterns of (1) graphite and (2) GO; (b) XRD patterns of (1) GO, (2) iGO, (3) hiGO, (4) pGO and (5) hpGO.

The surface compositions and concentrations of different N-groups of all N-doped graphene nanoplatelets were further monitored by XPS (Figure 2). As shown in Figure 2 (a), the N 1s peaks in iGO, pGO, hiGO and hpGO are clearly detected at around 399 eV, indicating that incorporation of nitrogen via ketoamine condensation reactions is successful. Compared with hiGO and hpGO, the O 1s peaks at about 532 eV in iGO and pGO are more prominent, which are in accordance with the surface composition analysis. The atomic ratios of O atom in iGO and pGO are 18.24% and 14.18% (Table 1), respectively, while those of hiGO and hpGO are 2.24% and 2.86% (Table 2), respectively, which are consistent with the fact that GO can be reduced by thermal treatment to generate reduced GO with little oxygen content. The conductivity of hiGO and hpGO benefits from the reduction of oxygen content due to thermal treatment.

According to the principle of nitrogen doping in Scheme 1, iGO and pGO are supposed to possess –C=N- only in addition to unreacted amidogen of o-phenylenediamine, which is well confirmed by XPS of iGO and pGO (Figure 2 (b)), because there is only one N1s signal in either iGO or pGO. The peak area of pGO is bigger than that of iGO in Figure 2 (b), suggesting that nitrogen content is higher in pGO, which is also proved by the surface composition analysis. The nitrogen doping content of iGO is 3.37% which is much lower than 6.88% for pGO (Table 1).

It's widely accepted that four most pronounced styles of nitrogen species can be discriminated on the N 1s spectrum: quaternary or graphitic N (401.4 eV), pyrrolic N (400.5 eV), pyridinic N (398.6 eV), and pyridinic N+-O- (402-405 eV), respectively (Scheme 2) [15,17]. The locations of different N groups described above are illustrated in Scheme 2, three kinds of nitrogen species like pyrrolic N, pyridinic N and pyridinic N+-O- can only locate at the edge of graphene and are considered as 'edge-N'. Graphitic-N can insert into the carbon matrix and may be found on the edge, that is, it can act as both 'bulk-N' and 'edge-N'.

As shown in Scheme 1, -C=O bond can only exists at the edge of GO, so the generation of –C=N- bond is supposed to replace –C=O bond on site via the ketoamine condensation reactions between the ketone group of GO and amidogen of aniline. Therefore, unlike the traditional doping methods which are randomly due to uncontrollable carbonization and doping, GO doped in terms of –C=N- bond is supposed to obtain edge-selectively N-doped graphene nanoplatelets due to controllable carbonization of GO and high bond energy of –C=N- bond. Because the -C=N- bond in iGO and pGO is stable during the thermal treatment, so there is a little possibility to generate graphitic-N in 'edge-N' from -C=N- bond.

As shown in Figure 2 (c-d), the N 1s peaks are fitted to three dominant peaks at 400.91°, 397.98° and 404.15 for hiGO, and at 400.81°, 397.98° and 403.66° for hpGO (Table 2), which are assigned to pyrrolic-N, pyridinic-N, and pyridinic N+-O-, respectively, suggesting edge-selectively N-doped graphene materials without graphitic-N are obtained.

Electrochemical Properties

The reason that it is difficult to distinguish the catalytic role of each nitrogen form is that it is hard to separate graphitic nitrogen atoms from others via traditional methods due to randomness of doping. As mentioned above, edge-selectively N-doped graphene nanoplatelets without graphitic N, that is hiGO and hpGO, have been obtained via the ketoamine condensation reactions. Therefore, hiGO and hpGO were employed to discuss the role of 'edge-N' as metal free ORR catalysts.

As shown in Figure 3, hiGO shows the best performance in O_2-saturated 0.1 mol/L KOH solution at room temperature. Compared with the poor performance of GO, although iGO and hiGO are doped by nitrogen, the enhancement of activity is slight, suggesting that N doping at the edge of graphene without metal doping does not play an important role in ORR activity.

The same situation also applies to N-doped ORR catalysts based on pGO (Figure 4). hpGO shows the best performance. In contrast with pGO, thermal treatment enhances the conductivity of hpGO and contributes to the formation of aromatic rings at the edge of graphene, which are beneficial to improvement of performance. In addition, the nitrogen content of hiGO is 3.4% while that of hpGO is 4.28%. Among of them, pyrrolic-N in hiGO and hpGO accounts for 1.72% and 2.36%, pyridinic-N in

Table 1. Surface composition of iGO and pGO

	Peak BE	iGO Atom %	Peak BE	pGO Atom %
C 1s	284.63	78.39	284.6	78.94
O 1s	531.86	18.24	531.94	14.18
N 1s	399.86	3.37	398.84	6.88

Table 2. Surface composition and concentrations of different N-groups in hiGO and hpGO

	Peak BE	hiGO Atom %	Peak BE	hpGO Atom %
C 1s	284.61	94.26	284.61	92.82
O 1s	532.17	2.24	532	2.86
Pyrrolic-N	400.91	1.72	400.81	2.36
Pyridinic-N	397.98	1.08	397.98	1.3
Pyridinic-N+-O-	404.15	0.6	403.66	0.62

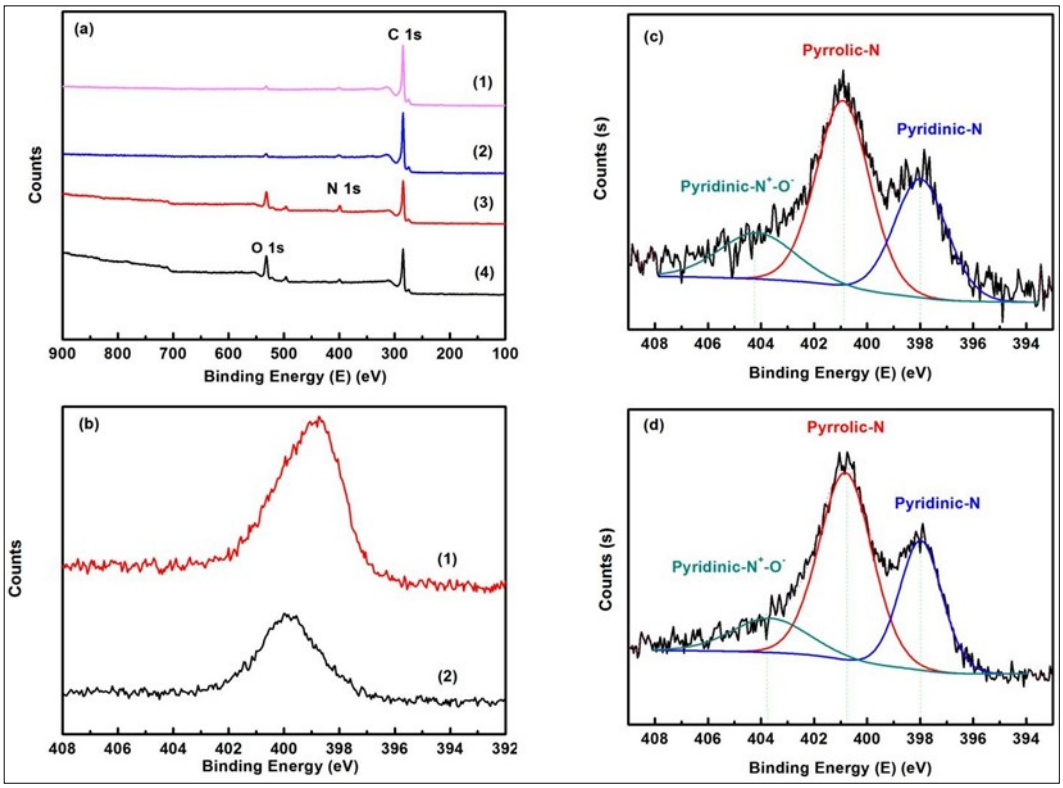

Figure 2. (a) Full XPS spectra of (1) hpGO, (2) hiGO, (3) pGO, (4) iGO; (b) XPS N 1s spectra of (1) pGO and (2) iGO; XPS N 1s spectra of hiGO (c) and hpGO (d).

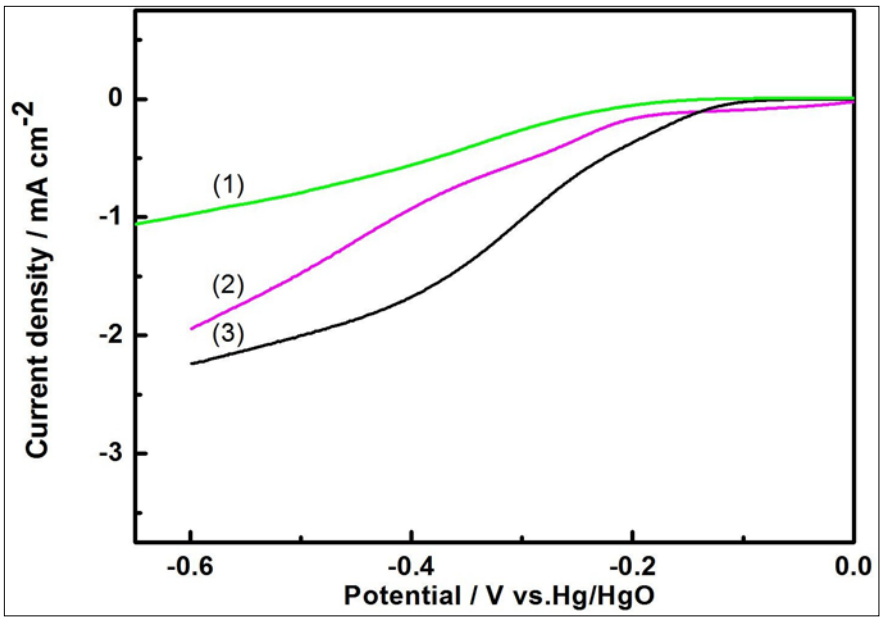

Figure 3. ORR polarization curves of (1) GO, (2) iGO and (3) hiGO in O_2-saturated 0.1 mol/L KOH. Potential range: from 0.1 V to -0.6 V vs. Hg/HgO electrode (1 M KOH). Scan rate: 5 mV s-1

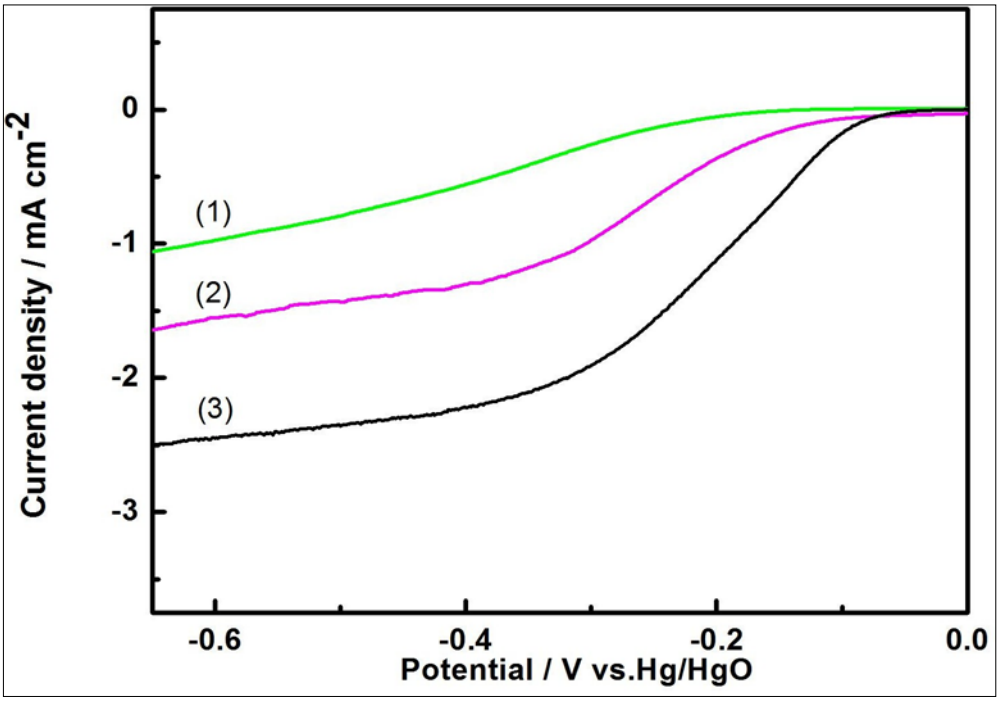

Figure 4. ORR polarization curves of (1) GO, (2) pGO and (3) hpGO in O_2-saturated 0.1 M KOH. Potential range: from 0.1 V to -0.6 V vs. Hg/HgO electrode (1 mol/L KOH). Scan rate: 5 mV s-1

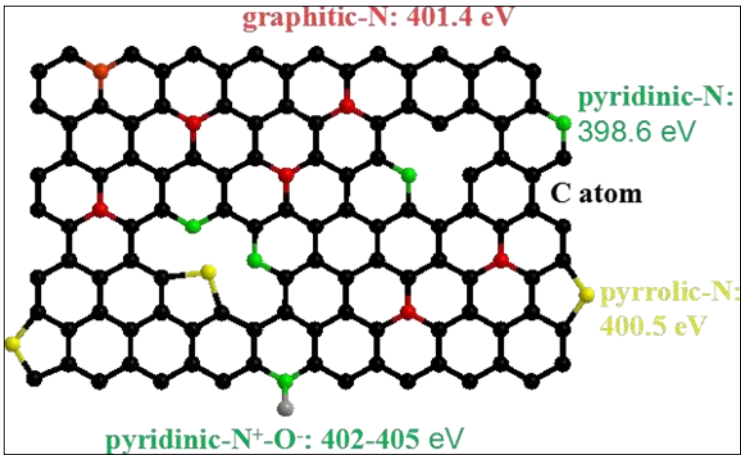

Scheme 2. Schematic illustration of nitrogen species with the corresponding reported XPS binding energies in the N-doped graphene. The black, red, green, yellow and gray spheres represent the C, graphitic N, pyridinic N, pyrrolic N and oxygen atoms in the N-doped graphene, respectively.

hiGO and hpGO accounts for 1.08% and 1.3%, respectively. The pyridinic-N with lone pair electrons is always considered as the ORR active site, which may make the difference in terms of performance of hiGO and hpGO. As metal free catalysts for ORR, the edge-selectively nitrogen-doped graphene nanopaltelets improve the ORR activity but the enhancement is not prominent, suggesting the 'edge-N' such as pyrrolic N, pyridinic N and pyridinic N+-O- don't play significant roles in ORR activity.

Conclusions

The process of N-doping was controlled precisely via ketoamine condensation reactions, and then N-doped graphene nanoplatelets with pyrrolic N, pyridinic N and pyridinic N+-O- rather than graphitic nitrogen were prepared by post thermal treatments, which are confirmed by XPS spectra. The nitrogen contents of N-doped graphene and N-doped GO are up to 4.28% and 6.88%, respectively. Although the improvement of ORR performance benefits from N-doping, the edge-selectively nitrogen doping does not play an important role on enhancement of ORR activity.

Funding

This work was supported by the National Natural Science Foundation of China (22172237, 21706293, 21503282), the China Scholarship Council, and the Fundamental Research Funds for the Central Universities South-Central University for Nationalities (CZY14005)

References

1. L. Dai, Y. Xue, L. Qu, H. J. Choi, J. B. Baek, Chem. Rev. 115 (2015) 4823-4892.
2. G. Wu, A. Santandreu, W. Kellogg, S. Gupta, O. Ogoke, H. Zhang, H. L. Wang, L. Dai, Nano Energy 29 (2016) 83-110.
3. C. Du, X. Gao, W. Chen, Chin. J. Catal. 37 (2016) 1049-1061.
4. H. Jin, J. Li, F. Chen, L. Gao, H. Zhang, D. Liu, Q. Liu, Electrochim. Acta 222 (2016) 438-445.
5. K. Gong, F. Du, Z. Xia, M. Durstock, L. Dai, Science 323 (2009) 760-764.
6. H. Kim, K. Lee, S. I. Woo, Y. Jung, Phys. Chem. Chem. Phys. 13 (2011) 17505-17510.
7. D. Yu, Q. Zhang, L. Dai, J. Am. Chem. Soc. 132 (2010) 15127-15129.
8. R. Liu, D. Wu, X. Feng, K. Müllen, Angew. Chem. 122 (2010) 2619-2623.
9. J. Tong, W. Li, L. Bo, W. Wang, Y. Li, T. Li, Q. Zhang, H. Fan, Chin. J. Catal. 39 (2018) 1138-1145.
10. X. Ge, A. Sumboja, D. Wuu, T. An, B. Li, F. W. T. Goh, T. S. A. Hor, Y. Zong, Z. Liu, ACS Catal. 5 (2015) 4643-4667.
11. J. Kong, W. Cheng, Chin. J. Catal. 38 (2017) 951-969.
12. D.W. Chang, E. K. Lee, E. Y. Park, H. Yu, H. J. Choi, I. Y. Jeon, G. J. Sohn, D. Shin, N. Park, J. H. Oh, L. Dai, J. B. Baek, J. Am. Chem. Soc. 135 (2013) 8981-8988.
13. G. Liu, B. Wang, L. Xu, P. Ding, P. Zhang, J. Xia, H. Li, J. Qian, Chin. J. Catal. 39 (2018) 790-799.
14. S. Liu, H. Zhang, Z. Xu, H. Zhong, H. Jin, Int J Hydrogen Energy 37 (2012) 19065-19072.
15. J. Liu, P. Song, M. Ruan, W. Xu, Chin. J. Catal. 37 (2016) 1119-1126.
16. Z. Xing, Y. Qi, Z. Jian, X. Ji, ACS Appl. Mater. Interface 9 (2017) 4343-4351.
17. Y. Wang, L. Dong, G. Lai, M. Wei, X. Jiang, L. Bai, Nanomaterials 9 (2019) 131-140.